Dislocation core radii near elastic stability limits

C. A. Sawyer, J. W. Morris, Jr., and D. C. Chrzan
Department of Materials Science and Engineering, University of California, Berkeley, California 94720, USA
(Received 28 January 2013; published 22 April 2013)

Recent studies of transition metal alloys with compositions that place them near their limits of elastic stability [e.g., near the body-centered-cubic (BCC) to hexagonal-close-packed (HCP) transition] suggest interesting behavior for the dislocation cores. Specifically, the dislocation core size is predicted to diverge as the stability limit is approached. Here a simple analysis rooted in elasticity theory and the computation of ideal strength is used to analyze this divergence. This analysis indicates that dislocation core radii should diverge as the elastic limits of stability are approached in the BCC, HCP, and face-centered-cubic (FCC) structures. Moreover, external stresses and dislocation-induced stresses also increase the core radii. Density functional theory based total-energy calculations are combined with anisotropic elasticity theory to compute numerical estimates of dislocation core radii.

DOI: 10.1103/PhysRevB.87.134106 PACS number(s): 62.20.fq, 81.40.Lm

I. INTRODUCTION

By now, the theoretical basis of plasticity in most metals is well in hand. Since the 1930s, the accepted mechanism for plastic deformation of most metals is motion of dislocations that takes place at stresses orders of magnitude below the ideal strength of the crystal.[1] The theoretical prediction of the plastic properties of metals, then, most often becomes an exercise in understanding the dynamics of the dislocations contained within the metal.

However, in 2003 researchers at Toyota introduced an interesting TiNb based alloy that they called gum metal.[2] This alloy displays a host of super properties including super strength (yield strength of approximately 1.2 GPa) and super elasticity (elastic limit over 2%). In addition, the alloy is ductile, and displays elongations of over 10% in simple tensile tests. Interestingly, the alloy displays no work hardening during those same tests. Even more interesting is the fact that these "super" properties fully emerge only after extensive cold working.

Remarkably, postdeformation examination of the microstructure in gum metal reveals few (if any) lattice dislocations. Instead, one observes "nanodisturbances," localized nanoscale distortions in the crystal that can be modeled as the strain field associated with nonlattice dislocations with small Burgers vectors.[3] The macroscopic plasticity appears to be mediated by slip of so-called "giant" faults,[2] a mechanism similar to that envisioned in theories of plasticity based on ideal strength.[4]

In fact, gum metal was designed to have an intrinsically low moduli difference, $C_{11} - C_{12}$. Since this difference governs the ideal shear strength of body-centered-cubic (BCC) metals, the ideal shear strength of gum metal is expected to be quite low. This understanding, when combined with the above experimental observations, led Saito *et al.* to conclude that bulk gum metals deform at their ideal strength without the need to move dislocations.[2]

Later observations of the deformation of solution treated gum metal did reveal the presence of dislocation mediated plasticity.[5] So there is no intrinsic materials property that prevents the formation of dislocations in these alloys. However, a necessary condition for (cold-worked) gum metal to deform at ideal strength without the motion of dislocations is that dislocations, if present, must be immobile, even under the influence of stresses as high as the ideal shear strength.

There are extrinsic and intrinsic materials properties that influence dislocation mobility. The presence of obstacles to dislocation glide can pin dislocations, and inhibit plasticity. Additionally, the structure of the dislocation core, i.e., that region of the crystal near the dislocation that cannot be described by continuum elasticity theory, can inhibit dislocation glide. For example, in BCC metals, it has been argued that a spread dislocation core leads to lower dislocation mobility.[6]

Based on studies of a TiV approximant to gum metal, it has been argued that dislocations within gum metal are easily pinned, even at stresses equal to predicted ideal shear strengths.[7] In addition, the dislocation cores within gum metal are expected to be spread over large distances.[8] So large, in fact, that dislocation cores may overlap yielding distortions similar to the experimentally observed "nanodisturbances," and making it difficult to resolve individual dislocations within transmission electron microscopy experiments. In the TiV approximants to gum metals, both the extended dislocation core radii and the easy pinning of dislocations are the result of approaching the limits of elastic stability of the BCC crystal structure.

This observation suggests an interesting avenue of exploration. If proximity to the elastic limit of the BCC phase leads to alloys with interesting "super" properties, can similar phenomena be observed at the limits of elastic stability for other crystal symmetries? Kuramoto *et al.* have considered this possibility, and have demonstrated that a face-centered-cubic (FCC) Fe-Ni-Co-Ti alloy engineered to be near the elastic limits of stability for the FCC structure displays behavior very similar to gum metal.[9] This paper addresses the issue by exploring dislocation core radii near the limits of elastic stability within the BCC, FCC, and hexagonal-close-packed (HCP) phases. Remarkably, the calculations suggest that as the elastic limit is approached, the cores of dislocations within all these structures will spread, and potentially behave similarly to dislocations within gum metal.

The next section discusses the definition of the dislocation core radius. The sections following address estimates for the dislocation core radii in various structures. More accurate estimates of dislocation core radii in specific materials can be obtained by combining electronic structure based calculations of ideal strength with linear anisotropic continuum elasticity theory. A formalism for doing so is presented in Sec. VI, and applied to Mo (as a prototypical BCC metal) in Sec. VII. Section VIII presents the conclusions.

II. DISLOCATION CORE RADII

Dislocations are marked by long-ranged stress and strain fields *and* local changes in bonding. The long-ranged stress and strain fields can be modeled very accurately using linear anisotropic continuum elasticity theory. (For the sake of brevity, unless noted otherwise, we henceforth define the phrase "elasticity theory" to refer to linear anisotropic continuum elasticity theory.) However, elasticity theory is fundamentally incapable of describing the dislocation near its origin, precisely where the changes in bonding are found.

More specifically, the dislocation within the elasticity theory is a singularity within the elastic field: The predicted stress and strain both diverge at the position of the dislocation. This singularity is, of course, nonphysical. Real crystalline materials are simply not an elastic continuum, particularly when viewed on scales for which one can resolve the individual atoms, and the stress and strain associated with a dislocation within a crystal does not diverge at the position of the dislocation. Nevertheless, the bulk of the dislocation's energy is stored in the long-ranged stress and strain field, and for this reason, elasticity theory forms the basis for much of our understanding of the properties of dislocations.

In dislocation applications, elasticity theory is augmented with the introduction of a core radius. Nominally, the core radius demarcates the boundary between the region of the crystal in which elasticity theory is applicable and the region where elasticity theory is inapplicable, a region known as the dislocation core. In practice, there is no set way to introduce the core radius. Hirth and Lothe suggest choosing the cutoff so that the computed elastic energy is roughly equal to the total energy of the dislocation.[1] This definition is convenient, particularly if one wants to model dislocation dynamics, as forces can be computed simply by considering changes in the elastic energy alone, but it does not allow one to estimate the true extent of the dislocation core.

Other choices of dislocation core radii may prove useful in other circumstances. Consider, for example, the dynamics of screw dislocations within BCC materials. Studies of these dislocations revealed that the bonding rearrangements associated with the dislocation core can extend a substantial distance from the core region.[6] Since movement of the dislocation requires reconfiguration of the bonding over extended regions of space in the spread dislocation core, these spread cores limit the mobility of the dislocations. Thus while elasticity theory can predict the driving force for dislocation motion, only an atomic scale theory can reveal the atomic scale motions that determine dislocation mobilities. Consequently, dislocation core studies have become a significant tool in the study of mechanical properties (see, for example, Refs. 8 and 10–12).

The calculation of dislocation core structures, however, is considerably complex. The long-ranged stresses and strains imply that boundary conditions impact atomic scale calculations.[13] Moreover, the small unit cells accessible to computation using electronic structure based total-energy methods rooted in density functional theory make dislocation/dislocation interactions a prominent part of many first-principles computational methods. As a result, dislocation core studies are frequently confined to a specific material, and extracting physical trends regarding core structures requires an expensive and painstaking computational approach.

There is reason, however, to seek a more rapid and general approach to ascertain the extent of the core region within a dislocation. Such an approach enables the identification of trends within classes of materials. Moreover, a more rapid general approach will enable a high throughput computational approach to discover materials with interesting mechanical properties, such as gum metal.

To address this need, consider the following definition of a dislocation core radius. In what follows, the dislocation core radius is defined as that radius for which the stress field of the dislocation that is predicted by elasticity theory equals the ideal strength of the material under the identical stress loading condition. More specifically, at each point in space (except the dislocation line itself), elasticity theory computes a stress tensor. If there is no crystal distortion that gives rise to the predicted stress tensor, then clearly elasticity theory has failed. Additionally, the computed stress is declared to exceed the ideal strength of the material. Conversely, if the predicted stress state can be attained through the imposition of some crystal distortion, the predictions of elasticity theory may well be accurate. The point nearest to the dislocation core in a particular radial direction for which the distortion can be found is a strict lower bound on the dislocation core radius, and for the purposes of this paper, is declared to be the dislocation core radius in that radial direction. By considering all radial directions, one can construct a polar plot of the dislocation core radius.

Consider, for example, the case of a pure screw dislocation within a BCC metal. The stress field is given by the simple expression[1,14] $\sigma_{z\theta} = \frac{Kb}{2\pi r}$, with $\mathbf{b}$ the Burgers vector. The stress field is cylindrically symmetric, with the z axis along the dislocation line, and only the $z\theta$ shear component is nonzero; the energy factor of the dislocation, K, depends on the elastic properties of the material and on the orientation of the dislocation. For BCC metals, the ideal strength may be regarded as a fraction of the shear modulus,[15] $\sigma_{\text{ideal}} = fG$, with G in the direction of shear and thus orientation dependent. (The shear modulus in the [111] direction of BCC alloys is independent of the shear plane.) The fraction f is also orientation dependent, as for instance the easy and hard directions of shear in the same plane will give very different ideal strengths. The core radius then is simply r_{core} such that $\sigma_{z\theta}(r_{\text{core}}) = fG$, or

$$r_{\text{core}} = \frac{b}{2\pi f}\frac{K}{G}. \tag{1}$$

For the $\mathbf{b} = \frac{a}{2}\langle 111\rangle$ screw dislocation in BCC metals, one finds[8]

$$r_{\text{core}} = \frac{b}{6\pi f}\sqrt{\frac{(C_{11}-C_{12}+4C_{44})\left(2C_{11}^2+2C_{11}C_{12}-4C_{12}^2+13C_{11}C_{44}-7C_{12}C_{44}+2C_{44}^2\right)}{3C_{44}(C_{11}-C_{12})(C_{11}+C_{12}+2C_{44})}}. \tag{2}$$

Note that this core radius diverges as $C_{11} - C_{12} \to 0$ or as $C_{44} \to 0$, two of the elastic stability limits of BCC crystals. This means that as varying the composition, for instance, of a BCC crystal brings it close to these elastic stability limits, the core radius defined here *diverges*. Interestingly, gum metals are designed to be near this limit. It is also interesting to note that a simple analysis relates the elastic constants to the observed easy pinning and extended dislocation core structures.

III. ESTIMATES OF DISLOCATION CORE RADII

A. Screw dislocation in FCC

Following Hirth and Lothe, the energy coefficient for a screw dislocation in FCC[1] is $K = \sqrt{c'_{44}c'_{55} - c'^2_{45}}$, where c'_{ij} denotes the components of the stiffness tensor rotated into a basis with its three-axis along the dislocation line. The Burgers vector and dislocation line for the most common screw dislocation are in a $\langle 110 \rangle$ direction, giving

$$K = \sqrt{\tfrac{1}{2}(C_{11} - C_{12})C_{44}}$$

in the coordinates of the cubic crystal axes. The shear modulus in this direction depends on the shear plane; as a function of rotating the shear plane about the dislocation line (where $\theta = 0$ is a $\{1\bar{1}0\}$ plane) is

$$G_{\langle 110 \rangle} = \frac{C_{44}(C_{11} - C_{12})}{2C_{44}\cos^2\theta + (C_{11} - C_{12})\sin^2\theta}$$

and the dislocation core radius in the sense of the ideal strength is

$$r_{\text{core}} = \frac{b}{2\sqrt{2}\pi f}\frac{2C_{44}\cos^2\theta + (C_{11} - C_{12})\sin^2\theta}{\sqrt{(C_{11} - C_{12})C_{44}}},$$

which diverges as $C_{11} - C_{12} \to 0$ or as $C_{44} \to 0$. Unlike the expression for BCC, this depends strongly on the angle around the dislocation. For shear on the (001) plane, the core radius goes to zero instead of diverging as $C_{11} - C_{12} \to 0$, and on the $(1\bar{1}0)$ plane the radius goes to zero as $C_{44} \to 0$. Discussion of these special planes will be deferred to Sec. V. The most common slip plane in FCC, $\{111\}$, is at about 35° in this scheme; the core radius on the slip plane diverges for both criteria.

It should be noted that in real crystals, dislocations are often split into partials;[1] this effect has not been considered in this work, but the core radii of partial dislocations could readily be calculated by the same means, using the appropriate line direction and nonlattice Burgers vector.

B. Screw dislocation in HCP

The energy coefficient for an HCP screw dislocation[1] is $K = \sqrt{c'_{44}c'_{55}}$ in coordinates with the three-axis aligned with a screw dislocation on the common slip system, a $\langle 11\bar{2}0 \rangle$ direction, and the one-axis also in the basal plane. In the standard coordinates, with the three-axis perpendicular to the basal plane, this becomes $K = \sqrt{C_{44}C_{66}}$. The shear modulus on $\langle 11\bar{2}0 \rangle$ depends on the shear plane,

$$G_{\langle 11\bar{2}0 \rangle} = \left(\frac{\cos^2\theta}{C_{44}} + \frac{\sin^2\theta}{C_{66}}\right)^{-1},$$

where $\theta = 0$ is shear on the basal plane. The dislocation core radius is

$$r_{\text{core}} = \frac{b}{2\pi f}\frac{C_{66}\cos^2\theta + C_{44}\sin^2\theta}{\sqrt{C_{44}C_{66}}}.$$

Since in the hexagonal crystal $C_{66} = \frac{1}{2}(C_{11} - C_{12})$, this expression is the same as the FCC case, and diverges as $C_{11} - C_{12} \to 0$ or as $C_{44} \to 0$. The same special planes are observed; $C_{11} - C_{12} \to 0$ does not lead to divergence on the basal plane, and $C_{44} \to 0$ does not cause a divergence perpendicular to the basal plane.

IV. EDGE AND MIXED DISLOCATIONS

In edge and mixed dislocations, the stress has both tensile and shear components, and a tensor version of the energy coefficient is needed to describe the stress state,[14]

$$\begin{aligned}
\sigma_{r\theta} &= [(K_{11}b_1 + K_{12}b_2 + K_{13}b_3)\cos\theta \\
&\quad + (K_{21}b_1 + K_{22}b_2 + K_{23}b_3)\sin\theta]/2\pi r, \\
\sigma_{\theta\theta} &= [(K_{21}b_1 + K_{22}b_2 + K_{23}b_3)\cos\theta \\
&\quad - (K_{11}b_1 + K_{12}b_2 + K_{13}b_3)\sin\theta]/2\pi r, \\
\sigma_{z\theta} &= (K_{31}b_1 + K_{32}b_2 + K_{33}b_3)/2\pi r,
\end{aligned}$$

where $\mathbf{K}$ and $\mathbf{b}$ are referred to rectilinear axes with the three-axis along the dislocation, and (r,θ,z) are cylindrical coordinates with z aligned with the dislocation line and $\theta = 0$ at the one-axis. These three stress components must be compared to the relevant (shear or tensile) ideal strength, which depends on the dislocation orientation and on θ. This leads to multiple core radii at each angle; the outer envelope of these core radii as a function of angle gives the effective core radius.

Although for some high-symmetry directions an analytical form of $\mathbf{K}$ can be found, a simple expression does not generally exist, so it is more practical to solve for the core radius numerically. $\mathbf{K}$ can be found for an arbitrary dislocation using the Stroh theory.[16] Following the method laid out by Hirth and Lothe,[1] in brief, a parenthesis operator

$$(ab)_{jk} = a_i C_{ijkl} b_l$$

is introduced, where $\mathbf{a}$ and $\mathbf{b}$ are any vectors, and $\mathbf{C}$ is the stiffness tensor. Two vectors $\mathbf{m}$ and $\mathbf{n}$ are introduced which form a right-handed coordinate system with the dislocation line, and a matrix

$$\mathbf{N} = \begin{Bmatrix} -(nn)^{-1}(nm) & -(nn)^{-1} \\ -[(mn)(nn)^{-1}(nm) - (mm)] & -(mn)(nn)^{-1} \end{Bmatrix}$$

is constructed, where each entry is a three-by-three block. This matrix has six eigenvalues p_α and eigenvectors $\zeta_\alpha \equiv \{A_{1,\alpha}, A_{2,\alpha}, A_{3,\alpha}, L_{1,\alpha}, L_{2,\alpha}, L_{3,\alpha}\}$, normalized such that $2\mathbf{A}_\alpha \cdot \mathbf{L}_\alpha = 1$. The energy tensor is then

$$\mathbf{K} = i\sum_{\alpha=1}^{6} \pm \mathbf{L}_\alpha \otimes \mathbf{L}_\alpha,$$

where the sign of each term in the sum is chosen to be the same as the sign of the imaginary part of the corresponding eigenvalue. The resulting $\mathbf{K}$ tensor is referred to the same basis as the elastic constants used, meaning it must be rotated

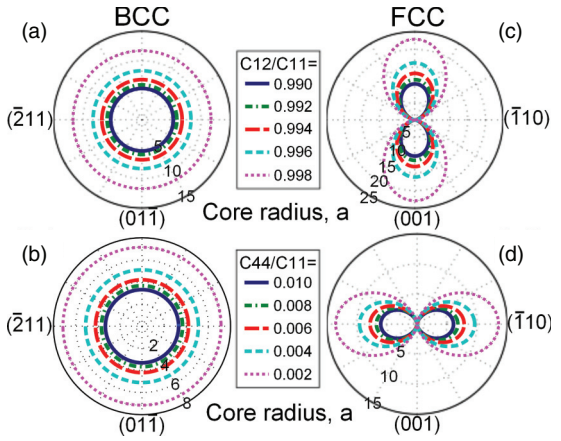

FIG. 1. (Color online) Polar plots illustrating the dislocation core region as the elastic constants approach critical values. The dislocation line (and Burgers vector) is at the origin and perpendicular to the page. The $b = \frac{1}{2}[111]$ screw dislocation in BCC as (a) $C_{11} - C_{12} \to 0$ and (b) $C_{44} \to 0$, and the $b = \frac{1}{2}[110]$ screw dislocation in FCC as (c) $C_{11} - C_{12} \to 0$ and (d) $C_{44} \to 0$. The ideal strength used here is set to $0.11G$ at all angles for illustration purposes, $f = 0.11$ having been found by Krenn *et al.* (Ref. 15) for the easy directions of shear in BCC metals. The horizontal axis shows the dependence on angle around the dislocation, which is notably absent in BCC due to the high symmetry of the modulus in the [111] direction. For (a) and (c), $C_{44}/C_{11} = 0.5$, while for (b) and (d), $C_{12}/C_{11} = 0.3$.

into the dislocation basis used in the stress expressions given above.

V. DIVERGENCE CRITERIA

BCC, FCC, and HCP crystals all have divergences as $C_{11} - C_{12} \to 0$ and as $C_{44} \to 0$ for both screw (see Fig. 1) and edge dislocations. These two conditions for divergence are two of the criteria for elastic stability which arise from the energy condition $\delta E = \delta(\frac{1}{2}V_0 C_{ij}\varepsilon_i\varepsilon_j) > 0$. Cubic crystals have the additional criterion that $C_{11} + 2C_{12} > 0$, and hexagonal crystals that $(C_{11} + C_{12})C_{33} - 2C_{13}^2 > 0$. Although these other criteria do not lead to divergences in the core radius for screw dislocations, they do for edge dislocations: FCC and BCC edge dislocations have divergent core radii as $C_{11} + 2C_{12} \to 0$ and HCP edge dislocations diverge as $(C_{11} + C_{12})C_{33} - 2C_{13}^2 \to 0$. These results are summarized in Table I.

Except for the screw dislocation in BCC, all core radii depend strongly on the angle. Figure 1 shows the angle dependence in FCC, including planes on which the core radius goes to zero. All dislocations in FCC and HCP, and one of the common BCC edge dislocations, have special planes for which the core radius goes to zero or remains finite at the instabilities. These special planes are all low-index planes, and several are the slip planes of the crystal, including all the special planes as $C_{11} + 2C_{12} \to 0$ or $(C_{11} + C_{12})C_{33} - 2C_{13}^2 \to 0$. The significance of these planes is not entirely clear; in principle, elasticity theory works until very close to the dislocation on these planes. On the other hand, if the core of the dislocation undergoes reconstruction, the displacement of nearby off-plane atoms will likely create stresses on the atoms on the special planes.

Not all dislocations in a material will be pure screw or lowest-energy edge dislocations; all mixed and edge dislocations with the same Burgers vector have been analyzed. All edge and mixed dislocations in BCC, FCC, and HCP structures have divergent dislocation core radii at all three stability criteria; special planes appear in some high-symmetry directions. In BCC, the group of edge and mixed dislocations with $b = \frac{a}{2}[111]$ and $\xi = [11l]$, where l is any constant, all have finite core radii on the slip plane $(1\bar{1}0)$ as $C_{11} + 2C_{12} \to 0$. Two special mixed dislocations in this group are $\xi = [001]$, which also has a finite core radius on $(1\bar{1}0)$ as $C_{44} \to 0$, and $\xi = [110]$, which has a finite core radius on $(1\bar{1}0)$ as $C_{11} + 2C_{12} \to 0$ and on (001) as $C_{44} \to 0$.

In FCC, three similar groups exist with $b = \frac{a}{2}[110]$ and $\xi = [11l]$, $\xi = [1\bar{1}l]$ or $\xi = [hk0]$; these dislocations have finite radii as $C_{11} + 2C_{12} \to 0$ on $(1\bar{1}0)$, $(1\bar{1}\frac{2}{l})$, or (001), respectively. This includes the most common edge dislocation, with $\xi = [1\bar{1}2]$, on the $(1\bar{1}\bar{1})$ slip plane. Other special dislocations within these groups are $\xi = [001]$, which also has a finite core radius on $(1\bar{1}0)$ as $C_{44} \to 0$; $\xi = [1\bar{1}0]$, which is finite on (001) as $C_{11} - C_{12} \to 0$; and $\xi = [100]$, which remains finite on (001) as $C_{11} - C_{12} \to 0$ and on (010) as $C_{44} \to 0$.

TABLE I. Summary of results for edge and screw dislocations in three crystal structures. Rows labeled with a stability criterion indicate whether the core radius diverges at that criterion. Rows labeled "Special planes" indicate any planes for which the radius remains finite. *For HCP, this is not a stability criterion; instead the analogous $(C_{11} + C_{12})C_{33} - 2C_{13}^2 \to 0$ is used.

	BCC			FCC		HCP	
Structure Type	Screw	Edge		Screw	Edge	Screw	Edge
b	$\frac{1}{2}[111]$	$\frac{1}{2}[111]$	$\frac{1}{2}[111]$	$\frac{1}{2}[110]$	$\frac{1}{2}[110]$	$[11\bar{2}0]$	$[11\bar{2}0]$
ξ	$[111]$	$[11\bar{2}]$	$[5\bar{4}\bar{1}],[1\bar{1}0]$	$[110]$	$[1\bar{1}2]$	$[11\bar{2}0]$	$[1\bar{1}00]$
$C_{11} - C_{12} \to 0$	yes	yes	yes	yes	yes	yes	yes
Special planes	none	(111)	none	$(1\bar{1}0)$	none	$(1\bar{1}00)$	(0001)
$C_{44} \to 0$	yes	yes	yes	yes	yes	yes	yes
Special planes	none	none	none	(001)	none	(0001)	$(1\bar{1}00)$
$C_{11} + 2C_{12} \to 0$*	no	yes	yes	no	yes	no*	yes*
Special planes	N/A	$(1\bar{1}0)$	none	N/A	$(1\bar{1}\bar{1})$	N/A	(0001)

In HCP, with $b = \frac{a}{2}[11\bar{2}0]$, the group $\xi = [1\bar{1}0l]$ has special planes on $(1\bar{1}0\frac{2}{l})$ as $(C_{11} + C_{12})C_{33} - 2C_{13}^2 \to 0$ and on $(11\bar{2}0)$ as $C_{44} \to 0$. The group $\xi = [hk\overline{(h+k)}0]$ has special planes on (0001) as $(C_{11} + C_{12})C_{33} - 2C_{13}^2 \to 0$. The prismatic edge dislocation, with $\xi = [0001]$, cannot be calculated by the numeric method given above, but the energy coefficient K_e is given by Hirth and Lothe[1] as

$$K_e = \frac{C_{11}^2 - C_{12}^2}{2C_{11}},$$

which leads to stresses

$$\sigma_{r\theta} = \frac{K_e b \cos\theta}{2\pi r},$$
$$\sigma_{\theta\theta} = \frac{K_e b \sin\theta}{2\pi r},$$

while the relevant moduli are $G = (\frac{2}{C_{11}-C_{12}})^{-1}$ for shear and

$$E = \left(\frac{-C_{13}^2 + C_{11}C_{33}}{(C_{11} - C_{12})\left[-2C_{13}^2 + (C_{11} + C_{12})C_{33}\right]}\right)^{-1}$$

for tension. Thus the core radius is the maximum of the radii given by the shear and tensile criteria,

$$r_{\text{core,shear}} = \frac{b\cos\theta}{2\pi f}\frac{C_{11} + C_{12}}{C_{11}},$$

$$r_{\text{core,tensile}} = \frac{b\sin\theta}{4\pi f}\frac{(C_{11} + C_{12})\left(C_{11}C_{33} - C_{13}^2\right)}{C_{11}\left[(C_{11} + C_{12})C_{33} - 2C_{13}^2\right]}.$$

This leads to divergence in the core radius as $C_{11} \to 0$ from both shear and tension, so there are no special planes. When $(C_{11} + C_{12})C_{33} - 2C_{13}^2 \to 0$, the core diverges due to the tensile criterion only and the radius on the slip plane remains finite.

VI. IDEAL STRENGTH

The premise of the approach presented here is that if continuum linear elasticity theory predicts that the stress at a point exceeds the ideal strength of the material, then that point must be, by definition, within the dislocation core. In the discussion above, we used simple empirical relations between the ideal strength and the elastic moduli to argue that dislocation core radii diverge as one approaches the elastic stability limits of a given structure. This approximate discussion can be improved by computing more accurately the ideal strength entering the comparison.

More specifically, we can compute the dislocation core radii as follows. We begin by computing the stress state for a given point predicted by anisotropic linear continuum elasticity theory. We then use density functional theory based electronic structure total-energy calculations to determine if it is possible for a uniformly strained crystal to attain the predicted stress state. If a uniformly strained crystal can attain the predicted stress state, the point in question is outside of the dislocation core. Otherwise, the point is within the dislocation core. Polar plots of the dislocation core radius can be obtained by considering points along rays emanating from the core position normal to the dislocation line direction. Starting far from the core, one can easily find the necessary strain state using elasticity theory. As one approaches the core, nonlinear elastic effects, fully reflected in the electronic structure based total-energy calculation, become more important. Eventually one finds the point nearest to the core along this ray for which the uniformly applied stress can be sustained, and this is defined to be the dislocation core radius along the direction of the considered ray. Note that there is no need to compute the structure of the dislocation core, nor are there any artifacts of periodic boundary conditions to consider. The detailed numerical procedure is described below.

Molybdenum was chosen as a test material because it is an elemental BCC metal with fairly high strength. Calculations are performed using the QUANTUM ESPRESSO package[17] and the pseudopotential Mo.pw91-n-van.UPF from http://www.quantum-espresso.org for molybdenum. The plane-wave energy cutoff used is 450 eV, a $9 \times 9 \times 9$ unsymmetrized k-point mesh is used, and the smearing scheme is Fermi-Dirac with a smearing constant of 0.01 Ry. These parameters converge the total energy to within 30 meV/atom. The elastic parameters and lattice constant are somewhat sensitive to the simulation parameters, so instead of using literature values, these are calculated using the same cutoff, smearing and k-point grid. The calculated values are $C_{11} =$ 430 GPa, $C_{12} = 154$ GPa, and $C_{44} = 90$ GPa, and the lattice parameter is 3.1885 Å. These are reasonably close to the values of 460, 176, and 110 GPa, respectively, given by Hirth and Lothe.[1] The elastic constants are calculated by applying strains between -2% and 2%, calculating the total energy, and fitting a parabola to the result, following the method of Fast *et al.*[18] adapted to cubic crystals. The stress cannot be directly imposed in simulation; instead, a strain is imposed, and the stress is calculated by QUANTUM ESPRESSO. The strain is then adjusted to minimize the difference between the calculated stress and the desired stress calculated by continuum elasticity theory. This is equivalent to stress control, as the strain is changed until the stress reaches the desired value. Minimization is performed with respect to the independent components of the strain using a standard Nelder-Mead simplex search.[19] The metric used for minimization is $f = \sum_{i=1}^{6}(\sigma_{QE,i} - \sigma_{el,i})^2$, where σ_{QE} is the stress calculated by QUANTUM ESPRESSO and σ_{el} is the stress predicted by linear elasticity theory. The minimized error in the stress is calculated for several test radii, chosen such that at least three or four test points are expected to be within the core region. Outside the core region, the minimization routine is expected to find a strain configuration that produces the predicted stress, and the error will be a small random value independent of radius. Inside the core radius, the minimization routine will find the maximum stress the crystal can sustain, independent of radius; since the predicted stress is proportional to $1/r$,

$$\sqrt{f_{\text{in}}} = \frac{c_1}{r} - c_2,$$

where c_1 and c_2 are radius-independent constants, related to K and the ideal strength, which can be discovered by a least-squares fit of the test data. Because it is not known *a priori* which data points fall within the core and which do not, an additional fitting parameter is used, $\sqrt{f} = \max(c_3, \frac{c_1}{r} - c_2)$, where c_3 represents the small random error outside the

core. The core radius is r such that $\sqrt{f_{\text{in}}(r)} = 0$, $r_{\text{core}} = \frac{c_1}{c_2}$. This process is then repeated for several angles around the dislocation, since the ideal strength is in general anisotropic. Crystalline symmetries, such as the threefold symmetry around a $\langle 111 \rangle$ direction in BCC, may be used to reduce the number of angles which must be calculated separately.

In addition to the properties of the core of a single dislocation isolated in an infinite medium, dislocations under various applied stresses are of interest and are accessible to this calculation method. The predicted stress simply becomes the sum of the stress due to the dislocation and the externally applied stress, whatever that may be. One case of particular interest is a uniform applied stress, which simulates the effect for instance of performing macroscopic mechanical tests on the dislocation-containing sample. Another interesting case is simulating the effects of nearby dislocations by adding the stresses they produce. This procedure will lend insight into the case of very high dislocation density, which may be expected for instance in gum metal, which must be heavily cold worked before its most interesting properties emerge.[2]

VII. CORE RADII IN REAL MATERIALS

The calculated elastic constants for molybdenum are $C_{11} = 430$ GPa, $C_{12} = 154$ GPa, and $C_{44} = 90$ GPa, and the lattice parameter is 3.1885 Å. For a screw dislocation, this leads to $K = 119$ GPa and $G = 117$ GPa, and a core radius of 4.0539 Å using the easy-direction ideal strength $\sigma_{\text{ideal}} = 0.11G$ found by Krenn *et al.*[15] The ratio K/G, which Chrzan *et al.* propose as a measure of the elastic anisotropy, is 1.01, very close to the isotropic value of 1.

The calculated core structure is shown in Fig. 2. The core radius on the easy directions of shear on $\{110\}$ and $\{112\}$ planes is between 3.29 and 3.38 Å. In the hard direction on $\{112\}$, the radius is smaller, as expected, at 2.90 Å. On planes other than the $\{110\}$ and $\{112\}$ slip planes, the radius is close to that on the easy directions. These calculations correspond to an ideal strength in the easy directions of roughly $0.13G$, and in the hard direction on $\{112\}$ $\sigma_{\text{ideal}} \approx 0.15G$. Error estimated from varying the starting point of the simplex search is roughly ± 0.2 Å.

Figure 2 also shows the effect of applying a homogeneous external shear stress. In general, homogeneous applied stresses serve to shift the dislocation core and expand it due to the $1/r$ dependence of the predicted stress. For a single dislocation embedded in an infinite crystal, the core expands with applied shear stress until, at the ideal strength applied, half the crystal can be considered core; at still higher applied stresses the only noncore region would be a small oblong where the applied stress and the stress from the dislocation cancel out. Of course, a real crystal would fail well before this point, either by moving the dislocation or some other mechanism.

Figure 3 shows the effect of adding the stress due to an adjacent dislocation with either the same or opposite sign. The second dislocation is placed 10 Å away; this would represent an unreasonably high dislocation density, but was chosen to give a large effect for illustration purposes. Screw dislocations of the same sign create stresses of opposite sign between them, causing the stress to cancel out and the cores to shrink in this region. On the far side of each dislocation, the stresses add and the core expands; the net area of the dislocation core increases. On the other hand, two dislocations of the opposite sign create stresses that add in the region between them, and cancel on the far side of either dislocation. This leads to a shift and stretching of the core towards the other dislocation, and an overall increase in the core area. At this close spacing, the two dislocation cores would overlap on the line between them, creating one large dislocation core region. In both cases—same sign or opposite sign dislocations—the dislocation cores expand.

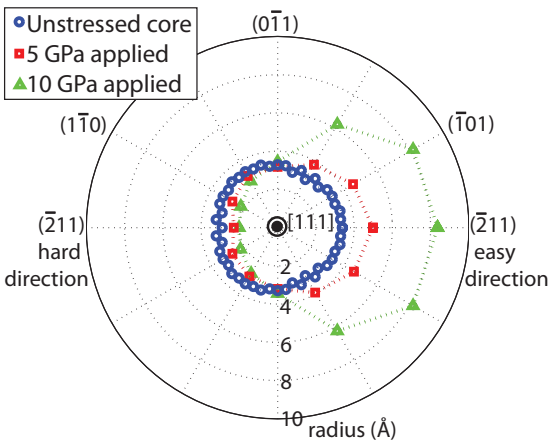

FIG. 2. (Color online) Polar plot of the dislocation core region in molybdenum. Dotted lines serve only as a guide for the eye. The circles (blue online) show the dislocation core with no applied stress. The squares (red online) are under a uniform applied stress of 5 GPa on the ($\bar{2}$11) plane in the [111] direction. The triangles (green online) are under a stress of 10 GPa in the same configuration. As the uniform applied stress increases, the core expands and shifts towards the side where the applied stress and stress due to the dislocation have the same sign.

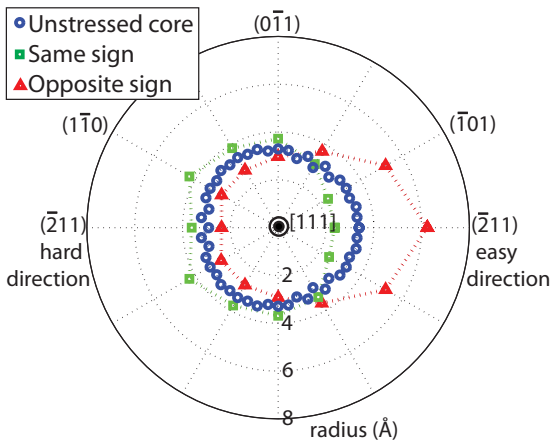

FIG. 3. (Color online) Polar plot of the dislocation core region in molybdenum. Dotted lines serve only as a guide for the eye. The circles (blue online) show the dislocation core with no applied stress. The squares (green online) are calculated under the influence of a nearby dislocation with the same Burgers vector, and the triangles (red online) with the opposite Burgers vector (or opposite line sense). The other dislocation in both cases is placed 10 Å away, parallel to the first dislocation, on the right-hand side of the ($\bar{2}$11) plane in the figure.

These results suggest two ways to increase the core size extrinsically; both applying a stress and increasing the dislocation density will cause cores to expand. At high enough applied stresses and dislocation densities, cores overlap; at still higher stresses or dislocation densities, these overlapping core regions spread throughout the crystal. Both of these methods assume stationary dislocations; mobile dislocations will move or annihilate and reduce their core area. However, a high K/G ratio leads to effective pinning of dislocations,[7] as well as larger cores. Raising the K/G ratio by manipulating the elastic constants, applying stresses, and/or raising the dislocation density work together to increase the dislocation core size.

VIII. CONCLUSIONS

Using continuum linear elasticity theory and atomistic simulations, we have identified three methods of increasing the dislocation core size in metals. The first is to modify the elastic constants via alloying or other methods; as crystals of BCC, FCC, or HCP structures approach the elastic stability limits, their dislocation cores grow. The second is to apply an external stress, which results in net growth of the cores. The third is to increase the dislocation density via cold-working or other methods; adjacent dislocations increase each other's core size whether they are the same or opposite-sign dislocations. Because large dislocation cores are found in gum metal, and are linked to some of the super properties,[7,8] it is hoped that driving other materials towards larger core sizes will produce new materials with similar properties.

ACKNOWLEDGMENT

This work was supported by the National Science Foundation under Grant No. DMR-1105081.

[1] J. P. Hirth and J. Lothe, *Theory of Dislocations*, 2nd ed. (Krieger, Malabar, Florida, 1982).
[2] T. Saito, T. Furuta, J.-H. Hwang, S. Kuramoto, K. Nishino, N. Suzuki, R. Chen, A. Yamada, K. Ito, Y. Seno, T. Nonaka, H. Ikehata, N. Nagasako, C. Iwamoto, Y. Ikuhara, and T. Sakuma, Science **300**, 464 (2003).
[3] Mikhail Yu. Gutkin, Toshitaka Ishizaki, Shigeru Kuramoto, and Ilya A. Ovid'ko, Acta Mater. **54**, 2489 (2006).
[4] J. Frenkel, Z. Phys. **37**, 572 (1926).
[5] E. Withey, M. Jin, A. Minor, S. Kuramoto, D. C. Chrzan, and J. W. Morris, Jr., Mater. Sci. Eng. A **493**, 26 (2008).
[6] V. Vitek, R. C. Perrin, and D. K. Bowen, Philos. Mag. **21**, (1970).
[7] T. Li, J. W. Morris, Jr., N. Nagasako, S. Kuramoto, and D. C. Chrzan, Phys. Rev. Lett. **98**, 105503 (2007).
[8] D. C. Chrzan, M. P. Sherburne, Y. Hanlumyuang, T. Li, and J. W. Morris, Jr, Phys. Rev. B **82**, 184202 (2010).
[9] S. Kuramoto, T. Furuta, N. Nagasako, and Z. Horita, Appl. Phys. Lett. **95**, 211901 (2009).
[10] Sohrab Ismail-Beigi and T. A. Arias, Phys. Rev. Lett. **84**, 1499 (2000).
[11] X. Xu, S. P. Beckman, P. Specht, D. C. Chrzan, R. P. Erni, I. Arslan, N. Browning, A. Bleloch, and C. Kisielowski, Phys. Rev. Lett. **95**, 145501 (2005).
[12] S. P. Beckman and D. C. Chrzan, Phys. B: Condens. Matter **340–342**, 990 (2003).
[13] M. S. Daw, Comput. Mater. Sci. **38**, 293 (2006).
[14] A. K. Head, Phys. Status Solidi **6**, 461 (1964).
[15] C. R. Krenn, D. Roundy, J. W. Morris, Jr., and M. L. Cohen, Mater. Sci. Eng. A **319–321**, 111 (2001).
[16] A. N. Stroh, Philos. Mag. **3**, 625 (1958).
[17] P. Giannozzi *et al.*, J. Phys.: Condens. Matter **21**, 395502 (2009).
[18] L. Fast, J. M. Wills, B. Johansson, and O. Eriksson, Phys. Rev. B **51**, 17431 (1995).
[19] J. C. Lagarias, J. A. Reeds, M. H. Wright, and P. E. Wright, Siam J. Optim. **9**, 112 (1998).